

# Muon performance with CMS detector in Run-2 of LHC

---

**Carlo Battilana\*** on behalf of the CMS Collaboration

*Università di Bologna ed Istituto Nazionale di Fisica Nucleare (INFN) - Sezione di Bologna,  
viale Bertini Pichat 6/2 - 40127 - Bologna, Italy.*

*E-mail:* [carlo.battilana@cern.ch](mailto:carlo.battilana@cern.ch)

The Compact Muon Solenoid (CMS) detector is one of the two multi-purpose experiments at the Large Hadron Collider (LHC) and has a broad physics program. Many aspects of this program depend on our ability to trigger, reconstruction, and identify events with final state muons in a wide range of momenta, from a few GeV to the TeV scale. In this talk, we present the full reconstruction procedure for both offline and online muons used in CMS. Additionally, identification and isolation strategies to discriminate prompt muons from those arising from background processes are described, and their performance is measured using 13 TeV data collected by the CMS experiment. Finally, the performance on benchmark channels will be shown.

*European Physical Society Conference on High Energy Physics - EPS-HEP2019 - 10-17 July, 2019, Ghent, Belgium*

---

\*Speaker.

## 1. Introduction

The second CERN Large Hadron Collider (LHC) run (Run-2), lasted from 2015 to 2018. During Run-2, LHC provided proton-proton collisions at a centre of mass energy up to 13 TeV, and operated at instantaneous luminosities up to  $\sim 2.2 \cdot 10^{34} \text{ cm}^{-2}\text{s}^{-1}$ . The Compact Muon Solenoid (CMS) experiment was able to collect a total integrated luminosity around  $150 \text{ fb}^{-1}$  of such high-energy collisions. The collected data sample allows CMS to probe physics beyond the standard model (BSM) and electroweak scale physics with unprecedented accuracy. Many of the performed analyses involve muons with a transverse momentum ( $p_T$ ) that spans a range from a few GeV to approximately 2 TeV. For this reason, an efficient muon trigger system as well as a precise muon reconstruction and identification are essential tools for the CMS experiment.

## 2. Offline and online muon reconstruction

The reconstruction and identification of muons in CMS is documented in [1]. It is performed using both the inner tracker, covering the innermost region of the detector and immersed in a 3.8 T solenoidal magnetic field, and a total of four layers of muon stations, positioned inside the steel return yoke surrounding the magnet. CMS features a silicon inner tracker consisting of pixel and strips detectors which covers a pseudorapidity region ( $\eta$ ) up to  $|\eta| = 2.5$ . The CMS muon system is equipped with gaseous detectors covering  $|\eta| < 2.4$ . Drift Tubes (DT) are used in the spectrometer barrel ( $|\eta| < 1.2$ ) whereas Cathode Strip Chambers (CSC) are used in the end-caps ( $0.9 < |\eta| < 2.4$ ). Both are tracking devices with standalone trigger capabilities. They are complemented by Resistive Plate Chambers, covering  $|\eta| < 1.9$ , which are primarily used in the trigger.

In the initial stage of the muon reconstruction, hit clusters (pixel, tracker, and RPC) or segments (DT, and CSC) are built independently within the different detectors. They are then combined to form tracks separately in the inner tracker (*tracker tracks*) and in the muon system (*standalone tracks*). For standalone tracks, a refit, which assumes that a muon originates from the interaction point is performed to improve the measure of the muon  $p_T$ . Starting from standalone tracks, matching with tracker tracks is attempted by propagating the two to a common surface, testing their compatibility, and selecting the pair whose tracker parameters are closest out of multiple potential combinations. For matched pairs, a combined track fit is performed to build a, so called, *global muon*. Additionally, tracker tracks, whose  $p_T$  exceeds a minimal threshold, are propagated to the muon system to look for potential matching with one or more DT or CSC segments. In case of a successful matching, a *tracker muon* is produced. A set of dedicated high-energy refits, aiming at combining information from the inner tracker and the muon chambers in a way that maximises the accuracy of the  $p_T$  measurement, is also run for muons with a  $p_T > 200 \text{ GeV}$  [1]. Global and tracker muons are complemented with quantities defining the quality of reconstructed objects (e.g. the  $\chi^2$  of a track fit, the multiplicity of tracker/muon hits used to build a track, etc ...) and muons are fed into the Particle Flow (PF) reconstruction [2]. Additionally, isolation, defined as the sum of energy deposits from either quantities from the inner detectors (tracker and calorimeters), or from PF objects (charged/neutral hadrons and photons), is computed in cones surrounding the muon. Identification criteria for use in physics analyses are defined from the track quality variables, isola-

tion, and requirements on the proximity of a muon track impact parameter to the primary vertex of the hard interaction.

The CMS trigger is organized in two stages. Firstly, a Level-1 Trigger (L1T) system, implemented using custom electronics, runs on coarse information from the calorimeters and the muon system and is able to reduce the data collection rate from 40 MHz (the LHC bunch-crossing frequency) to, at most, 100 kHz. At a second stage, a High-Level Trigger (HLT) runs a streamlined version of the CMS offline reconstruction algorithms on a computer farm consisting of commercial CPUs. It exploits full granularity information from all CMS detectors (i.e. inner tracker included) and provides a further reduction of the acquisition rate to approximately 1 kHz. Standalone muons built at HLT (L2) are essentially identical to the ones built offline, the main difference between the two being that L2 muons are requested to geometrically match L1T muon track candidates. The reconstruction of global and tracker muons at HLT evolved significantly throughout Run-2. In 2015 and 2016 three algorithms were run in *cascade*, from the fastest to the slowest. The starting point was the standalone muon at L2, and the cascade was stopping as soon as one of the algorithm built an HLT global muon track (L3), reconstructed with dedicated code for tracker track building. General purpose single and double muon triggers built relying on L3 reconstruction, were complemented by additional ones using tracker muons reconstructed at HLT [1]. In 2017, a complete overhaul of the L3 reconstruction was performed. Based on two sequences run in cascade, it makes muon tracking at HLT exploit the most up to date code used to build tracker tracks (*Iterative Tracking* [2]) and includes the reconstruction HLT tracker muons directly within the L3 track building. Finally, muon isolation is also computed at the HLT to discriminate prompt muons from the ones originating within QCD processes and constrain trigger rates.

### 3. Performance during the LHC Run-2

Various aspects of the performance of offline and online muon reconstruction, measured using both simulations and data collected by CMS during the LHC Run-2, are documented in [3] and [4]. A *tag-and-probe* method, exploiting dimuons from  $Z$  decays, is used to compute the online and offline muon efficiencies in samples of real data collected with single muon triggers. Within the method, a muon is defined as a *tag muon* if it fulfills stringent identification criteria and is geometrically matched with the trigger. Instead, the definition of the *probes* depends on the component of the muon selection that is measured (e.g. reconstruction/identification or isolation) and is chosen to avoid biases in the measurement. A probe is considered efficient if it fulfills the selection criteria under study. Figure 1 shows the reconstruction and identification efficiency measured with the tag-and-probe for the loosest (left) and tightest (centre) muon selection criteria typically used by CMS analyses (described in [1]). The first plot shows that the muon reconstruction efficiency is close to 100% both in simulations and data. The second one shows an average efficiency of 97%, that varies as function of the muon  $\eta$ . The dips in efficiency around  $|\eta| \sim 0.3$  correspond to the transition region between the central wheel of the muon spectrometer barrel and the neighbouring ones, covered by a smaller number of muon stations with respect to the rest of the system. Results for data and simulations show disagreement at the level of 3% or less (details about the origin of the disagreement are given in [1]). The muon trigger efficiency is computed with the same method (Fig. 1 - right). In this case, an average efficiency of  $\sim 90\%$  is found, with inefficiencies being

dominated by muon reconstruction at L1T and HLT isolation cuts. The black and blue dots refer to muon HLT efficiency computed respectively before and after a few optimizations to the L3 reconstruction were applied during the 2018 run (details in [4]).

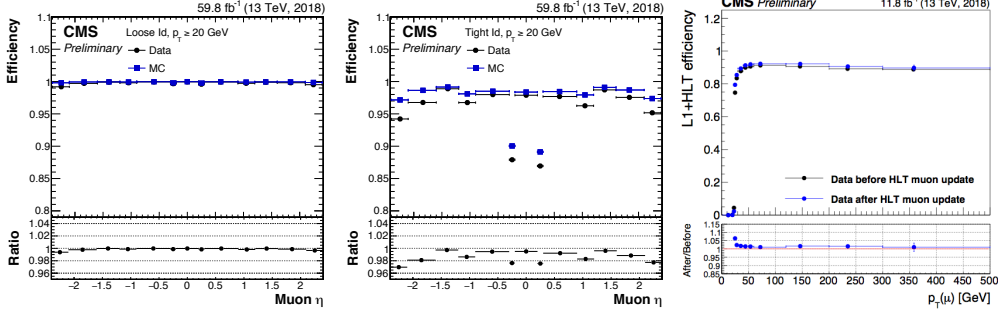


**Figure 1:** Muon reconstruction and identification efficiency for the *loose* (left) and *tight* (centre) identification criteria, as well as muon trigger efficiency (right), computed using the tag-and-probe method.

An accurate calibration of the muon  $p_T$  scale and resolution, valid for energies up to  $\sim 200$  GeV, is computed using dimuons from  $J\psi$  and  $Z$  boson decays. The  $1/p_T$  distribution of muons from  $Z$  bosons, as well as the known position of  $J\psi$  and  $Z$  resonance peaks, is used to derive additive and multiplicative correction factors to the muon curvature, which are computed in bins of muon charge,  $\eta$  and  $\phi$ . Additive corrections account for residual misalignments in the inner tracker, that are not fully corrected by the tracker alignment workflows. Multiplicative corrections are due to inaccuracy in the modeling of the magnetic field and the energy loss of muons traversing the inner tracker. Muon resolution dependence as function of  $\eta$  and  $p_T$  is also computed using the width of the invariant mass distributions and smearing factors are extracted to make simulations match real data. Figure 2 shows the impact of muon momentum scale and resolution calibration on a sample of dimuons dominated by Drell-Yan decays.

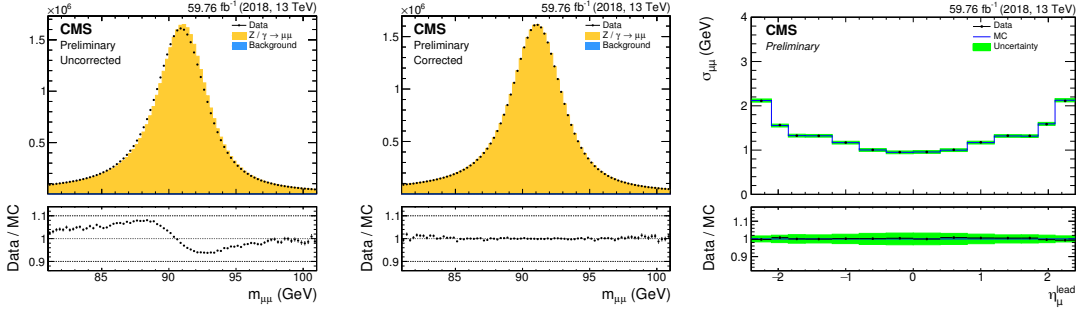


**Figure 2:** Invariant mass distribution (and its width) for a sample of dimuons dominated by  $Z$  decays computed before (left) and after (centre, right) momentum scale and resolution corrections are applied.

The performance of muons with energies of  $O(100)$  GeV or more was also studied in detail. For example, cosmic ray muons crossing CMS from top to bottom, and traversing the detector in a region close to its centre, can be used to measure the muon momentum resolution. The measurement is performed computing the relative  $q/p_T$  difference between of the muon tracks reconstructed separately in the “top” and “bottom” halves of the detector. Results from such mea-

surement are shown in Fig. 3 (left). The improvement at high  $p_T$  coming from the use of combined high-energy refits is visible from the figure. Biases in the scale of high-momentum muons, arising from inaccurate measurement the track curvature, are investigated using the *generalized endpoint* method. In this method, dimuon pairs are selected, and the  $q/p_T$  of muons with a  $p_T$  of at least 100 (200) GeV is plotted in bins for data and simulation, obtaining a distribution as the one in Fig. 3 (centre). Such distribution falls rapidly for small curvatures, and, in case of no scale biases, it is expected to have a kinematic endpoint at 0. In presence of additive curvature biases due to misalignment, the  $q/p_T$  distribution gets shifted and the kinematic endpoint moves away from 0. The accuracy of the scale measurement in data is measured by injecting curvature biases to the  $q/p_T$  distribution obtained from data, and comparing the resulting distribution with the (unbiased) one obtained from simulation by means of  $\chi^2$  test. The  $\chi^2$  is then computed as function of the injected scale bias and the bias value for data is obtained by minimizing such  $\chi^2$  distribution. Figure 3 (right) summarizes the results of the scale biases, computed in bins of  $\eta$  and  $\phi$ .

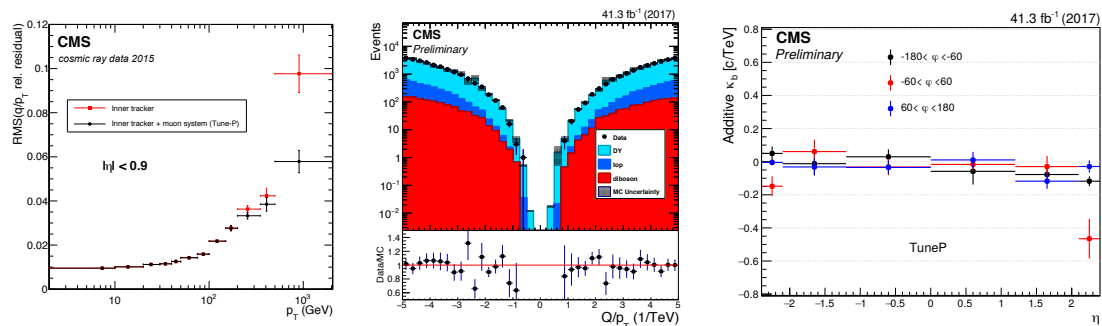


**Figure 3:** Muon momentum resolution computed using cosmic ray events (left). Muon momentum scale biases measured in proton-proton collisions using the generalized endpoint method (centre, right).

## 4. Summary

Muons are an element of prime importance to fulfill a large fraction of the CMS physics programme. Over the LHC Run-2, the online and offline muon reconstruction and identification performance was measured in all of its aspect and was found to be remarkably good. Overall performance from data agrees with simulations and, where relevant, high-level calibrations are computed to correct small discrepancies.

## References

- [1] The CMS Collaboration, “Performance of the CMS muon detector and muon reconstruction with proton-proton collisions at  $\sqrt{s} = 13$  TeV”, *JINST* **13** (2018), no.06, P06015.
- [2] The CMS Collaboration, “Particle-flow reconstruction and global event description with the CMS detector,” *JINST* **12** (2017), no.10, P10003.
- [3] The CMS Collaboration, “Muon reconstruction performance during Run II”, *CMS-DP-2019-022*, 2019.
- [4] The CMS Collaboration, “Muon HLT Performance with 2018 Data”, *CMS-DP-2018-034*, 2018.